Molecular Biology of the Cell
Vol. 9, 2477–2490, September 1998

Selective Perturbation of Apical Membrane Traffic by Expression of Influenza M2, an Acid-activated Ion Channel, in Polarized Madin–Darby Canine Kidney Cells

Jennifer R. Henkel,* Gerard Apodaca,* Yoram Altschuler,† Stephen Hardy,‡ and Ora A. Weisz*§

*Laboratory of Epithelial Cell Biology, Renal-Electrolyte Division, University of Pittsburgh, Pittsburgh, Pennsylvania 15261; †Department of Anatomy, University of California, San Francisco Medical School, San Francisco, California 94143; and ‡Cell Genesys, Foster City, California 94404

Submitted February 17, 1998; Accepted July 7, 1998
Monitoring Editor: Suzanne R. Pfeffer

The function of acidification along the endocytic pathway is not well understood, in part because the perturbants used to modify compartmental pH have global effects and in some cases alter cytoplasmic pH. We have used a new approach to study the effect of pH perturbation on postendocytic traffic in polarized Madin–Darby canine kidney (MDCK) cells. Influenza M2 is a small membrane protein that functions as an acid-activated ion channel and can elevate the pH of the *trans*-Golgi network and endosomes. We used recombinant adenoviruses to express the M2 protein of influenza virus in polarized MDCK cells stably transfected with the polymeric immunoglobulin (Ig) receptor. Using indirect immunofluorescence and immunoelectron microscopy, M2 was found to be concentrated at the apical plasma membrane and in subapical vesicles; intracellular M2 colocalized partly with internalized IgA in apical recycling endosomes as well as with the *trans*-Golgi network marker TGN-38. Expression of M2 slowed the rate of IgA transcytosis across polarized MDCK monolayers. The delay in transport occurred after IgA reached the apical recycling endosome, consistent with the localization of intracellular M2. Apical recycling of IgA was also slowed in the presence of M2, whereas basolateral recycling of transferrin and degradation of IgA were unaffected. By contrast, ammonium chloride affected both apical IgA and basolateral transferrin release. Together, our data suggest that M2 expression selectively perturbs acidification in compartments involved in apical delivery without disrupting other postendocytic transport steps.

INTRODUCTION

The plasma membrane (PM) of polarized cells is divided into apical and basolateral domains of distinct protein and lipid composition, which are separated by tight junctions. The polarized distribution of proteins and lipids is maintained by a combination of efficient sorting of newly synthesized proteins in the *trans*-Golgi network (TGN) and efficient segregation of endocytosed and transcytosed proteins in endosomal compartments. Although the TGN and endosomes are known to be acidified, the role of acidification in protein sorting by polarized cells is not well understood. Recent studies examining the effects of pH pertubation on endocytic traffic in nonpolarized cells have generated conflicting results. Many of these experiments used newly described inhibitors of the vacuolar H^+-

§ Corresponding author. E-mail address: weisz@med1.dept-med.pitt.edu.

[1] Abbreviations used: AMT, amantadine; ARE, apical recycling endosome; AV, adenovirus; Baf A_1, bafilomycin A_1; CMV, cytomegalovirus; DOX, doxycycline; HA, hemagglutinin; Ig, immunoglobulin; MDCK, Madin–Darby canine kidney; NOC, nocodazole; PBS-M, PBS containing 1 mM $MgCl_2$; pIgR, polymeric Ig receptor; PM, plasma membrane; Tf, transferrin; TGN, *trans*-Golgi network.

ATPase, such as bafilomycin A_1 (Baf A_1) or concanamycins A and B. For example, some groups have found that treatment with Baf A_1 does not affect the overall rate of endocytosis of either membrane or fluid phase markers (Clague *et al.*, 1994; Palokangas *et al.*, 1994). However, more recent detailed analysis suggests that in HepG2 cells, the rates of both endocytosis and recycling of transferrin (Tf) are reduced in the presence of Baf A_1 (van Weert *et al.*, 1995). Different groups have variously localized the block in transport to internalization or delivery to early endosomes (van Weert *et al.*, 1995), delivery from early to late endosomes (Clague *et al.*, 1994), recycling from late endosomes to the PM (van Weert *et al.*, 1995; Presley *et al.*, 1997), transport to lysosomes (van Weert *et al.*, 1995), or simply inhibition of degradation (Yoshimori *et al.*, 1991). It is not clear whether these different results are due to differences in the cell lines used, the tracers studied, or the methods used. Moreover, because the effects of Baf A_1 on transport are not readily reversible, some of the observed phenomena could be due to toxic side effects of drug treatment (Yilla *et al.*, 1993; van Weert *et al.*, 1995).

As an alternate approach, we have studied the effect of influenza M2 (Rostock strain) expression on postendocytic protein transport. M2 is a 97-amino acid nonglycosylated integral membrane protein encoded on RNA segment 7 of influenza virus (Lamb and Choppin, 1981). During synthesis, M2 is cotranslationally inserted into the endoplasmic reticulum and is transported to the PM of infected cells. The protein consists of a 24-amino-acid lumenal amino terminus, a single membrane-spanning domain, and a 54-amino-acid cytoplasmic tail. M2 forms a disulfide bonded tetramer that can conduct protons across artificial lipid bilayers and cell membranes when activated by low pH (Sugrue and Hay, 1991; Duff and Ashley, 1992; Pinto *et al.*, 1992). The anti-influenza drug amantadine (AMT) binds with high affinity to M2 and blocks its ion channel activity. Expression of M2 in Madin–Darby canine kidney (MDCK) cells has been demonstrated to elevate the pH of the *trans*-Golgi by ~0.8 pH units (Grambas and Hay, 1992). The cytoplasmic tail of Rostock M2 contains a sequence that closely resembles tyrosine-based motifs important for endocytosis, suggesting that this protein could be internalized after reaching the PM. Recently, Sakaguchi *et al.* (1996) demonstrated that M2 expression in nonpolarized cells decreases the kinetics of intracellular transport and cell surface delivery of newly synthesized proteins, consistent with previously documented effects of pH perturbation on biosynthetic transport (Muroi *et al.*, 1993; Yilla *et al.*, 1993; Palokangas *et al.*, 1994). However, unlike weak bases or vacuolar H^+-ATPase inhibitors, which affect the pH of all acidified organelles, M2 increases the pH of only those acidic compartments in which it is present and is therefore less likely to have global effects on transport. Furthermore, unlike Baf A_1, M2 activity can be rapidly and reversibly activated and blocked. Thus we reasoned that M2 expression would be a versatile tool with which to examine the role of acidification on postendocytic traffic in polarized cells.

We have used replication-defective recombinant adenoviruses to express M2 in polarized MDCK cells stably transfected with the polymeric immunoglobulin (Ig) receptor (pIgR) and examined its localization and effect on basolateral-to-apical transcytosis and apical recycling of IgA. Transcytosis of internalized IgA bound to the pIgR involves rapid microtubule-dependent passage from basolateral early endosomes to a subapical tubulovesicular compartment designated the apical recycling endosome (ARE) where intracellular IgA accumulates (Apodaca *et al.*, 1994). Upon delivery to the apical pole of the cell, the lumenal domain of pIgR is cleaved and released into the apical medium while still bound to ligand. A small proportion of apically delivered pIgR is not cleaved and recycles apically (Breitfeld *et al.*, 1989b). By indirect immunofluorescence and immunoelectron microscopy, we found M2 expression to be concentrated at the apical membrane and to a lesser extent in subapical compartments, including the ARE. Consistent with its localization, M2 expression had selective effects on apical delivery of preinternalized molecules. By contrast, treatment with the global pH perturbant ammonium chloride affected transport through both apical and basolateral compartments. Thus, M2 expression appears to be a useful tool with which to dissect the function of acidification in postendocytic transport to the apical surface.

MATERIALS AND METHODS

Cell Lines

Low-passage MDCK cells (type II) were maintained in MEM (Cellgro; Fisher Scientific, Pittsburgh, PA) supplemented with 10% fetal bovine serum (Atlanta Biologicals, Norcross, GA), streptomycin (100 μg/ml), and penicillin (100 U/ml). Generation and characterization of the MDCK T23 cell line, which stably expresses the tetracycline-repressible transactivator (Gossen and Bujard, 1992), is described by Barth *et al.* (1997). These cells also express the pIgR under control of the butyrate-inducible cytomegalovirus (CMV) promoter. By indirect immunofluorescence, >90% of the cells express detectable levels of pIgR after overnight induction with 2 mM butyrate. For all experiments, cells were seeded at high density (~2×10^5 cells per well) in 12-mm transwells (0.4-μm pore; Costar, Cambridge, MA) for 2–3 d before infection with recombinant adenovirus. Experiments were performed the following day.

Recombinant Adenoviruses

The vector pAdtet was generated by replacing the CMV promoter of pAdlox (Hardy *et al.*, 1997) with the minimal CMV promoter fused to the tetracycline operator (Gossen and Bujard, 1992). A *Bam*HI fragment containing the coding sequence for Rostock M2 (cDNA provided by Dr. Robert Lamb, Northwestern University, Evanston,

IL) was subcloned into pAdtet behind the tetracycline operon, and orientation of the inserts was determined by sequencing using primers homologous to regions upstream and downstream of the pAdtet multiple cloning site. DNA from individual clones encoding M2 in the correct and reverse orientations was isolated using the Jetstar maxiprep kit (Genomed, Research Triangle Park, NC), linearized with *Sfi*I, and transfected into CRE8 cells (Hardy *et al.*, 1997). E1-substituted recombinant adenoviruses encoding M2 in the correct and reverse orientations (AV-M2 and AV-M2rev, respectively) were generated using the method described by Hardy *et al.* (1997) and purified as described by Green and Pina (1963) with minor modifications (the cell lysate was not extracted with solvent, CsCl was used in place of RbCl, and the first gradient had two steps of 1.25 and 1.42 g/ml CsCl instead of a single step). Viral titer was estimated by measuring OD 260 nm of the final preparation and was typically 6×10^{12} particles/ml. Similar results were obtained with three independent preparations of AV-M2. A *Hin*dIII–*Not*I fragment containing the coding sequence of influenza hemagglutinin (HA; pCB6-HA_{Japan} provided by Dr. Michael Roth, University of Texas Southwest Medical Center, Dallas, TX) was subcloned into pAdtet and used to prepare a recombinant adenovirus encoding influenza HA (AV-HA).

Adenoviral Infection

Filter-grown MDCK T23 cells were washed by adding 3 ml calcium-free PBS containing 1 mM $MgCl_2$ (PBS-M) to the apical chamber and allowing it to spill over into the basolateral compartment. After 3–5 min at room temperature, the PBS-M was removed, and 150 μl PBS-M containing 0.2–10 μl recombinant adenovirus were added to the apical compartment (multiplicity of infection between 120 and 6000). The medium in the basolateral compartment was replaced with 0.5 ml PBS-M. The dishes were rocked briefly by hand, and the cells were returned to an incubator for 1–2 h. Mock-infected cells were treated identically, except that virus was omitted during the incubation period. Dishes were then rinsed with 2 ml PBS-M, and cells were incubated overnight in growth medium (1 ml apical, 1.5 ml basolateral). For most experiments, 2 mM sodium butyrate was added to induce expression of pIgR. pIgR expression in these cells was very low in the absence of butyrate induction. AMT (Sigma, St. Louis, MO; 5 μM), BL-1743 (a gift of Dr. Mark Krystal, Bristol-Myers Squibb Pharmaceutical Research Institute, Wallingford, CT; 5 μM) and doxycycline (DOX; Sigma; 20 ng/ml) were added as 1000-fold concentrated stocks prepared in 95% ethanol at this step or in subsequent steps where indicated to inhibit M2 activity or M2 expression, respectively.

Immunoprecipitation of Virally Expressed M2

Filter-grown MDCK T23 cells were infected with 2 μl AV-M2 or AV-M2rev as described above. The following day, cells were rinsed once with PBS, starved for 30 min in cysteine-free, methionine-free MEM containing 0.35 g/l $NaHCO_3$, 10 mM HEPES, and 10 mM 2-(*N*-morpholino)ethanesulfonic acid (pH 7.0) (medium A), and then radiolabeled in a humidified chamber for 2 h by placing the filters on a 25-μl drop of medium A containing 1.5 mCi/ml [^{35}S]Express (New England Nuclear, Boston, MA). After labeling, filters were rinsed once with PBS and then cut out of the plastic insert, and the cells were solubilized with 0.5 ml 60 mM octylglucoside and 0.1% SDS in HEPES-buffered saline containing aprotinin (1 μg/ml). Lysates were centrifuged for 7 min at 16,000 $\times$ *g* at room temperature, and the supernatants were immunoprecipitated with monoclonal 5C4, which is directed against the lumenal domain of M2 (a gift of Dr. Robert Lamb). Antibody–antigen complexes were collected using fixed *Staphylococcus aureus* (Pansorbin, Calbiochem, San Diego, CA) and washed three times with radioimmunoprecipitation assay buffer (10 mM Tris-HCl, 0.15 M NaCl, 1% Triton X-100, 1% Nonidet P-40, 0.1% SDS, pH 7.4). After elution in Laemmli sample buffer, samples were electrophoresed on 12% SDS-polyacrylamide gels, and the dried gel was placed under x-ray film (X-AR; Kodak, Rochester, NY).

Indirect Immunofluorescence and Laser Scanning Confocal Microscopy

Filter-grown T23 cells were fixed with paraformaldehyde using a pH shift protocol, quenched, blocked with 5% (vol/vol) goat serum, stained, mounted, and stored as described previously (Apodaca *et al.*, 1994). M2 expression was detected using mAb 5C4 (1:250 dilution), and HA was localized using mAb Fc125 (1:250; hybridoma cell line provided by Dr. Thomas Braciale, University of Virginia, Charlottesville, VA). The rat monoclonal antibody directed against ZO-1 (R40.76 hybridoma supernatant diluted 1:10) was included to localize tight junctions. Rabbit anti-human IgA (Jackson ImmunoResearch Laboratories, West Grove, PA; used at 10 μg/ml) was used to label internalized IgA in colocalization experiments. Primary antibodies were localized using appropriate FITC- or Cy-5-conjugated goat antibodies (Jackson ImmunoResearch). The samples were analyzed using a krypton–argon laser coupled to a Molecular Dynamics (Mountain View, CA) Multiprobe 2001 confocal scanner, attached to a Diaphot microscope (Nikon, Melville, NY) with a plan Apo 60×, 1.4 numerical aperture objective lens (Nikon). The samples were scanned using the appropriate filter combinations. Collection parameters were as follows: laser output, 65 mW; PMT-1 and PMT-2 set to 700–800 mV; laser attenuation, 10%; and 50-μm slit. The images (512 $\times$ 512 pixels, 0.08- to 0.17-μm pixel size) were acquired using ImageSpace software (Molecular Dynamics). The images were converted to tag-information-file format, and the contrast levels of the images were adjusted in the Photoshop program (Adobe, Mountain View, CA) on a Power PC Macintosh 9500 (Apple, Cupertino, CA). The contrast-corrected images were imported into Freehand (Macromedia, San Francisco, CA) and printed from a Kodak 8650PS dye sublimation printer.

Ultrathin Cryosectioning and Staining

MDCK T23 cells were cultured on 75-mm transwell filters, and after virus infection IgA was internalized from the basolateral pole of the cell for 10 min at 37°C. After three washes, the cells were chased in IgA-free medium for 5 min at 37°C. The cells were rinsed once with Dulbecco's PBS, fixed for 30 min at room temperature with 0.02% glutaraldehyde and 2% paraformaldehyde in PBS, scraped from the filter, and pelleted in a microfuge at 100 $\times$ *g*. The cell pellet was resuspended in an equal volume of 3% gelatin (200 bloom; Sigma) in PBS, incubated for 10 min at 37°C, and then placed on ice for 10 min to harden the gelatin. The gelatin–cell plug was cut into 0.5- to 1.0-mm^2 cubes, and the cubes were incubated overnight in 2.3 M sucrose and PBS at 4°C. The cubes were mounted on cryostubs and frozen in liquid nitrogen. Cryosectioning was performed at −110°C in an Ultracut E ultramicrotome with an FCS cryochamber attachment (Reichert, Buffalo, NY). The sections, collected on drops of sucrose, were transferred to butvar-coated nickel grids. Incubations were performed by inverting the grids on drops of the appropriate solution. The sections were incubated 15 min in PBS, washed three times for 5 min each with 0.15% (wt/vol) glycine and 0.5% (wt/vol) BSA dissolved in PBS (buffer 1), and then incubated for 20 min with 10% (vol/vol) goat serum diluted in buffer 1. The sections were incubated with 5C4 antibody (diluted in buffer 1) for 60 min at room temperature, washed three times for 5 min each with buffer 1, and then incubated with protein A-5 nm colloidal gold (purchased from Dr. Jan Slot, Utrecht University, Utrecht, the Netherlands) diluted in the same buffer for 30 min at room temperature. The sections were further washed three times for 5 min each with buffer 1, washed with PBS, fixed with 1.0% (vol/vol) glutaraldehyde (in PBS) for 5 min, rinsed with PBS, and then washed three times for 5 min each with buffer 1. The sections were then incubated with rabbit anti-human IgA for 60 min at room temperature, washed three times for 5 min each with buffer 1, and then incubated with protein A-10 nm

colloidal gold for 30 min at room temperature. The sections were further washed three times for 5 min each with buffer A, washed with PBS, fixed with 2.5% (vol/vol) glutaraldehyde (in PBS) for 5 min, rinsed with PBS and then water, stained with 2% (wt/vol) neutral uranyl acetate and 4% (wt/vol) aqueous uranyl acetate, and then embedded in 1.2% (wt/vol) methylcellulose. Sections were viewed at 80–100 kV in a Jeol (Tokyo, Japan) 100CX electron microscope.

Colocalization of Intracellular M2 and IgA

Filter-grown T23 cells were infected with AV-M2 as described above. The following day, cells were incubated with basolaterally added IgA (50 μg/ml) for 10 min at 37°C, washed three times, and then chased for 3 min at 37°C. Cells were subsequently rinsed twice with ice-cold medium B and then treated with *N*-tosyl-L-phenylalanine chloromethyl ketone–trypsin (200 μg/ml; Sigma) in medium B for 60 min on ice. Trypsinization was stopped by incubating twice for 10 min on ice with 400 μg/ml soybean trypsin inhibitor (Sigma). Cells were then fixed, permeabilized, and processed for indirect immunofluorescence to visualize M2, internalized IgA, and ZO-1.

Transcytosis and Recycling of IgA

IgA was radioiodinated using the iodine monochloride method to a specific activity of 1–2 $\times$ 10^7 cpm/μg (Breitfeld *et al.*, 1989a). Recycling and transcytosis assays were performed essentially as described by Maples *et al.* (1996). To measure IgA transcytosis, filter-grown MDCK T23 cells were rinsed with MEM/BSA (MEM, HBSS, 0.6% BSA, 20 mM HEPES, pH 7.4), and the bottom of the filter was blotted on a Kimwipe (Kimberly-Clark, Irving, TX) to remove excess medium. The filter insert was then placed on a 25-μl drop of MEM/BSA containing [^{125}I]IgA (~5 μg/ml), and ligand was internalized for 10 min at 37°C. The basal surface of the cells was rapidly washed rapidly three times and then once for 3 min, and the apical and basolateral media were aspirated and replaced with fresh medium (0.5 ml/compartment). At the designated time points, the apical and basolateral media were collected and replaced with fresh media. After the final time point, filters were cut out of the insert, and the amount of [^{125}I]IgA in all samples was determined using a gamma counter (Packard Instrument, Downers Grove, IL). An equal number of mock-infected MDCK cells not expressing the pIgR were treated identically to determine nonspecific IgA uptake and transcytosis, and these values were subtracted from those of the MDCK T23 cells. In some cases, the medium was trichloroacetic acid precipitated as described by Breitfeld *et al.* (1990) to determine the amount of IgA degraded and released into the apical and basolateral compartments during the experiment. Recycling of apically internalized IgA was performed as described above, except that [^{125}I]IgA diluted in 150 μl MEM/BSA was internalized for 30 min from the apical surface, and the apical compartment of the transwell was washed rapidly three times and then once for 3 min after ligand uptake.

Nocodazole Treatment

To examine the effect of M2 on the post-nocodazole (NOC)–sensitive step of transcytosis, T23 cells (mock infected or infected with AV-M2) were placed on a drop of MEM/BSA containing [^{125}I]IgA, and ligand was internalized for 10 min at 37°C. The basal surface of the cells was washed as described above. Cells were incubated at 37°C for 3 min to allow IgA accumulation in the apical recycling compartment (Apodaca *et al.*, 1994) and then rapidly chilled to 0°C and incubated for 30–60 min in the presence of 33 μM NOC (Calbiochem; prepared as a 1000-fold concentrated stock in DMSO), Subsequently, the cells were rapidly warmed to 37°C in the continued presence of NOC, and release of IgA into the medium was monitored as described above.

Tf Recycling Assays

Iron-saturated Tf (Sigma) was iodinated to a specific activity of 5–9 $\times$ 10^6 cpm/μg. Cells were depleted of intracellular stores of Tf by incubation for 1 h at 37°C in MEM/BSA. [^{125}I]Tf (~5 mg/ml) was internalized from the basolateral surface of cells for 45 min at 37°C. The cells were washed three times rapidly and twice for 5 min each with ice-cold MEM/BSA and then warmed to 37°C for 2.5 min to allow receptor internalization. The medium was replaced with 0.5 ml fresh MEM/BSA per compartment, and the postendocytic fate of [^{125}I]Tf was assessed as described above.

Treatment with Ammonium Chloride

Polarized MDCK T23 cells were incubated for 30 min at 37°C in MEM/BSA containing freshly dissolved ammonium chloride (Sigma) before internalization of [^{125}I]IgA or [^{125}I]Tf. Transcytosis and recycling assays were performed in the continued presence of either drug as described above.

RESULTS

Expression and Localization of M2 in Polarized MDCK Cells

To determine the effect of M2 expression on endocytic traffic, we infected polarized MDCK T23 cells using replication-defective recombinant adenoviruses encoding the Rostock strain of influenza M2. In this system, expression of M2 is dependent on the tetracycline transactivator stably expressed in the MDCK T23 cell line and can be inhibited by inclusion of DOX in the medium (Gossen and Bujard, 1992). To test the specificity and regulation of M2 expression using this system, we infected polarized MDCK T23 cells with recombinant adenoviruses encoding M2 in the correct (AV-M2) or reverse (AV-M2rev) orientation. After overnight incubation in the presence or absence of DOX or AMT, cells were radiolabeled, solubilized, and M2 immunoprecipitated using a monoclonal antibody (Figure 1). A labeled protein with an apparent molecular mass of ~18 kDa, consistent with the migration of M2 on SDS-PAGE gels, was immunoprecipitated from lysates of AV-M2-infected cells (Figure 1, M2). As expected, inclusion of AMT, which blocks M2 activity, did not affect M2 expression (Figure 1, M2+AMT). By contrast, inclusion of DOX, which inhibits transcription from the tet operon, completely blocked M2 expression (Figure 1, M2+DOX). No M2 was detected in lysates from mock-infected cells or cells infected with AV-M2rev (Figure 1, mock and M2rev lanes, respectively).

Subsequently, we localized M2 in polarized MDCK T23 cells using indirect immunofluorescence and immunoelectron microscopy. Filter-grown cells were infected with AV-M2, and the following day cells were fixed and processed for double-label indirect immunofluorescence using antibodies against M2 and the tight junction component ZO-1 (Figure 2). M2 was localized primarily to the apical surface of infected cells (Figure 2, A and B), although there was also

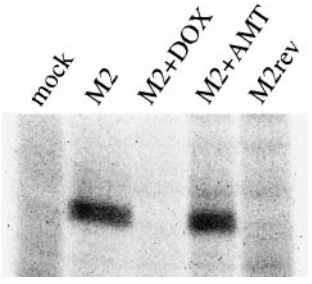

Figure 1. Adenoviral expression of Rostock M2 in polarized MDCK cells. MDCK T23 cells grown on filter inserts (12 mm diameter) were mock infected (mock) or infected for 60 min at 37°C with 2 μl AV-M2 (M2) or AV-M2rev (M2rev). DOX (20 ng/ml) or AMT (5 μM) was added to the medium immediately after removal of the virus. The following day, cells were starved for 30 min and pulse labeled for 2 h with [^{35}S]methionine in the continued presence of either DOX (M2+DOX) or AMT (M2+AMT). Filters were solubilized, the lysates were centrifuged briefly to remove debris, and M2 was immunoprecipitated. Samples were electrophoresed on a 12% SDS-polyacrylamide gel, and the dried gel was exposed to x-ray film.

staining of lateral and basal PMs (Figure 2, C and D). Adenoviral infection did not alter tight junction structure, because the localization of the tight junction component ZO-1 was normal in virally infected cells (Figure 2B, red). As a control to confirm that adenoviral infection did not compromise the polarity of MDCK cells, we assessed the cell surface distribution of influenza HA expressed using the recombinant adenovirus AV-HA. HA was localized almost exclusively to the apical surface of polarized MDCK T23 cells (Figure 2, E and F), and coexpression of HA with M2 did not qualitatively alter the distribution of either protein (Henkel and Weisz, unpublished results).

Because most of the M2 is present at the PM, it was difficult under our normal conditions to detect intracellular M2 using indirect immunofluorescence; therefore, we trypsinized the cell surface of polarized infected T23 cells to reveal the underlying intracellular M2. Trypsin treatment has previously been shown to cleave the extracellular domain of M2 (Zebedee *et al.*, 1985) and resulted in complete loss of M2 surface staining in nonpermeabilized cells. Initial experiments suggested that intracellular M2 was localized almost exclusively at the apical pole of cells, where the Golgi complex and apical endosomes are found. To determine whether intracellular M2 was present in the ARE, we internalized IgA from the basolateral surface of polarized cells for 10 min at 37°C, washed extensively, and then chased for 3 min at 37°C. It has previously been demonstrated that ~80% of internalized IgA is rapidly delivered to the ARE using this internalization protocol (the balance is in basolateral early endosomes [Apodaca *et al.*, 1996]). The cells were then rapidly chilled and treated with trypsin to remove cell surface M2. Samples were then fixed and

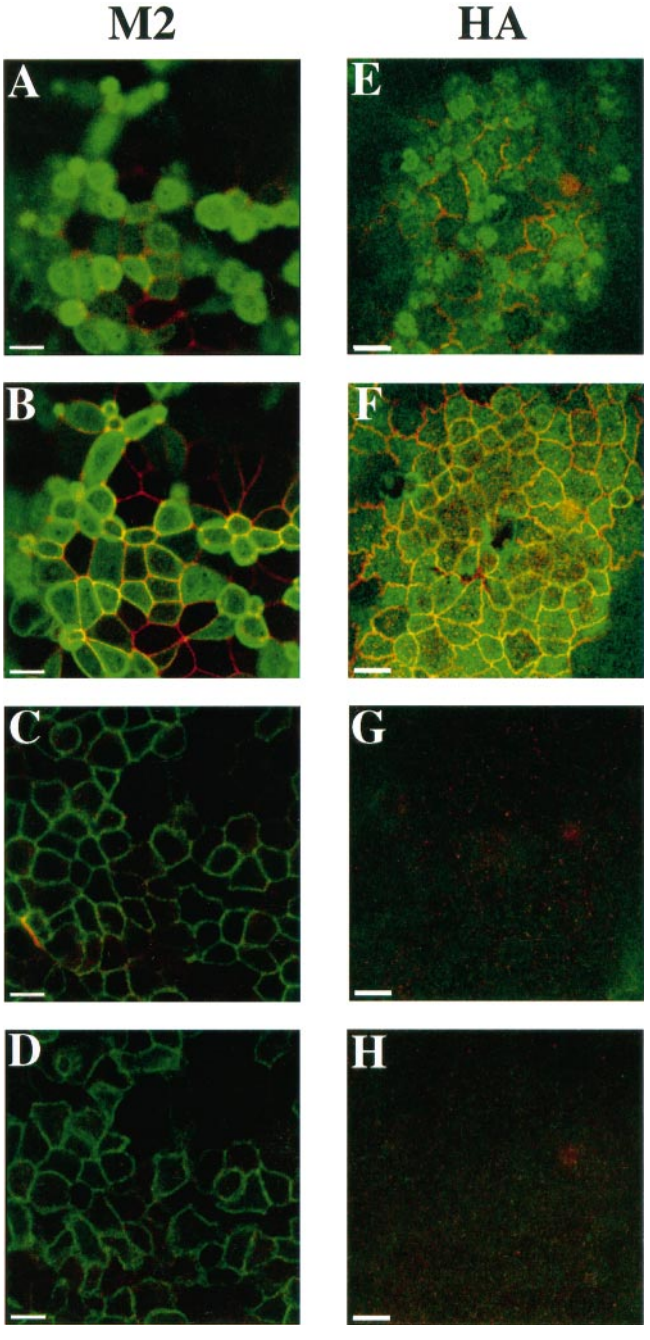

Figure 2. Localization of M2 and HA in polarized MDCK cells using indirect immunofluorescence. Polarized MDCK T23 cells were infected with AV-M2 (A–D) or AV-HA (E–H) as described in MATERIALS AND METHODS. The following day, cells were fixed, permeabilized, and double labeled using antibodies against ZO-1, a component of tight junctions (A–H, red), and either M2 (A–D, green) or HA antibody (E–H, green). Individual confocal sections taken from the apical surface (A and E), the level of the tight junction (B and F), the lateral surface (C and G), and the basal surface (D and H) are shown. Adenoviral infection does not disrupt the polarized morphology of the cells, because tight junction staining is normal, and HA is localized almost exclusively to the apical surface. By contrast, M2 is concentrated at the apical domain, but lateral and basal staining is also evident. Bars, 10 μm.

permeabilized, and IgA and M2 were detected using confocal microscopy (Figure 3). Intracellular M2 was localized primarily at the apical pole of the cells (Figure 3, E and F) with only faint staining found along the lateral and basal regions of the cell (Figure 3, G and H). The apically distributed M2 partly colocalized with IgA in the ARE (Figure 3, I and J). To a lesser extent, the small amount of M2 in the basolateral region of the cell occasionally colocalized with internalized IgA (Figure 3K, arrow). Moreover, M2 colocalized partly with internalized Tf in the apical but not the basolateral region of the cells. In addition, a small amount of the subapical M2 also colocalized with the TGN marker TGN-38; this population might represent newly synthesized M2 en route to the PM. Double-label immunoelectron microscopy confirmed colocalization of intracellular M2 with IgA in the ARE (Figure 4).

M2 Slows Transcytosis of IgA

Because intracellular M2 was concentrated in the ARE, we tested whether M2 expression affected transport through this compartment. To do this, we first monitored the effect of M2 on basolateral to apical transcytosis of IgA. Filter-grown MDCK T23 cells were infected with AV-M2 or AV-M2rev and then treated with 2 mM butyrate in the presence or absence of DOX. The next day, cells were incubated with basolaterally added [^{125}I]IgA at 37°C for 10 min. After washing to remove free [^{125}I]IgA, the appearance of [^{125}I]IgA in the apical medium was monitored. As shown in Figure 5A, expression of active M2 slowed the initial rate of [^{125}I]IgA release into the apical medium, although the amount of ligand eventually reaching the apical medium was only moderately decreased. By contrast, cells infected with AV-M2rev or AV-M2-infected cells treated with DOX to block M2 expression had normal rates of transcytosis, suggesting the effects were mediated by M2 expression. The effect of M2 was very reproducible and resulted in a 33% reduction in the initial rate of transcytosis (determined at the 15-min time point; $p < 0.0001$; $n = 9$) compared with mock-infected control cells. By contrast, the initial rate of transcytosis in AV-M2rev-infected cells or in AV-M2-infected cells treated with DOX or AMT was not distinguishable from mock-infected cells. Infection with 10 times more AV-M2 did not have a further effect on the rate of transcytosis, suggesting that inhibition of transcytosis was maximal under our standard conditions.

One explanation for the decreased rate of IgA transcytosis in M2-expressing cells could be increased dissociation of IgA from pIgR in alkalinized compartments. However, the transport of IgA in M2-expressing cells is profoundly different from the route of basolaterally internalized fluid phase markers, which are efficiently targeted to lysosomes and degraded (Bomsel *et al.*, 1989). By contrast, we found no significant difference in the amount of IgA degraded in control versus M2-expressing cells. Furthermore, we used a previously published method (Breitfeld *et al.*, 1990) to quantitate the kinetics of IgA dissociation from pIgR and found no difference in the rate or extent of IgA dissociation from pIgR measured at pH values between 6.0 and 7.2. Therefore, the inhibition of IgA transcytosis we observed likely reflects altered transport of the pIgR itself.

The decreased rate of IgA transcytosis in M2-expressing cells could be due directly to effects of M2 on the pH of endosomal compartments or to indirect consequences of prolonged M2 activity (in endosomes or other organelles) during the overnight postinfection period. To rule out the latter possibility, we examined the effect of acute activation of preaccumulated (inactive) M2 on IgA transcytosis (Figure 5B). To do this, we took advantage of a recently characterized inhibitor of M2 ion channel activity (BL-1743) whose effects are rapidly reversible upon washout (Tu *et al.*, 1996; Henkel and Weisz, 1998). Polarized MDCK T23 cells were infected with AV-M2, and some filters were incubated overnight with 5 μM BL-1743. The following day, the BL-1743 was washed out from half of the preincubated filters (Figure 5B, diamonds) for 30 min before IgA uptake (the half-time of M2 activation after BL-1743 washout is ~12 min [Tu *et al.*, 1996]). At this time, some filters that had expressed active M2 throughout the postinfection incubation were incubated with AMT to inactivate the M2. IgA transcytosis was monitored as described above. As expected, inclusion of BL-1743 throughout the transcytosis assays completely blocked M2-mediated inhibition of IgA transport (Figure 5B, upside-down triangles). Similarly, inhibition of active M2 by AMT addition immediately before the experiment completely restored IgA transcytosis (Figure 5B, triangles). By contrast, acute activation of M2 upon BL-1743 washout resulted in inhibition of IgA transcytosis, similar to cells expressing active M2 during the entire postinfection period (Figure 5B, compare squares and diamonds). To-

Figure 3 (facing page). Intracellular M2 partially colocalizes with internalized IgA in AREs. Filter-grown T23 cells infected with AV-M2 were allowed to internalize IgA from the basolateral side for 10 min at 37°C and then washed extensively and chased for 3 min to accumulate internalized IgA in the ARE. Cells were then chilled, trypsin-treated, fixed, permeabilized, and processed for indirect immunofluorescence. Individual confocal sections taken from the apical surface (A, E, and I), the level of the tight junction (B, F, and J), the lateral surface (C, G, and K), and the basal surface (D, H, and L) are shown. M2 (E–H) was localized using FITC-conjugated secondary antibody, and IgA and ZO-1 (A–D) were detected using Cy-5–conjugated secondary antibody. (I–L) Merged images. Arrows point to examples of structures in which M2 and IgA colocalize. Bar, 10 μm.

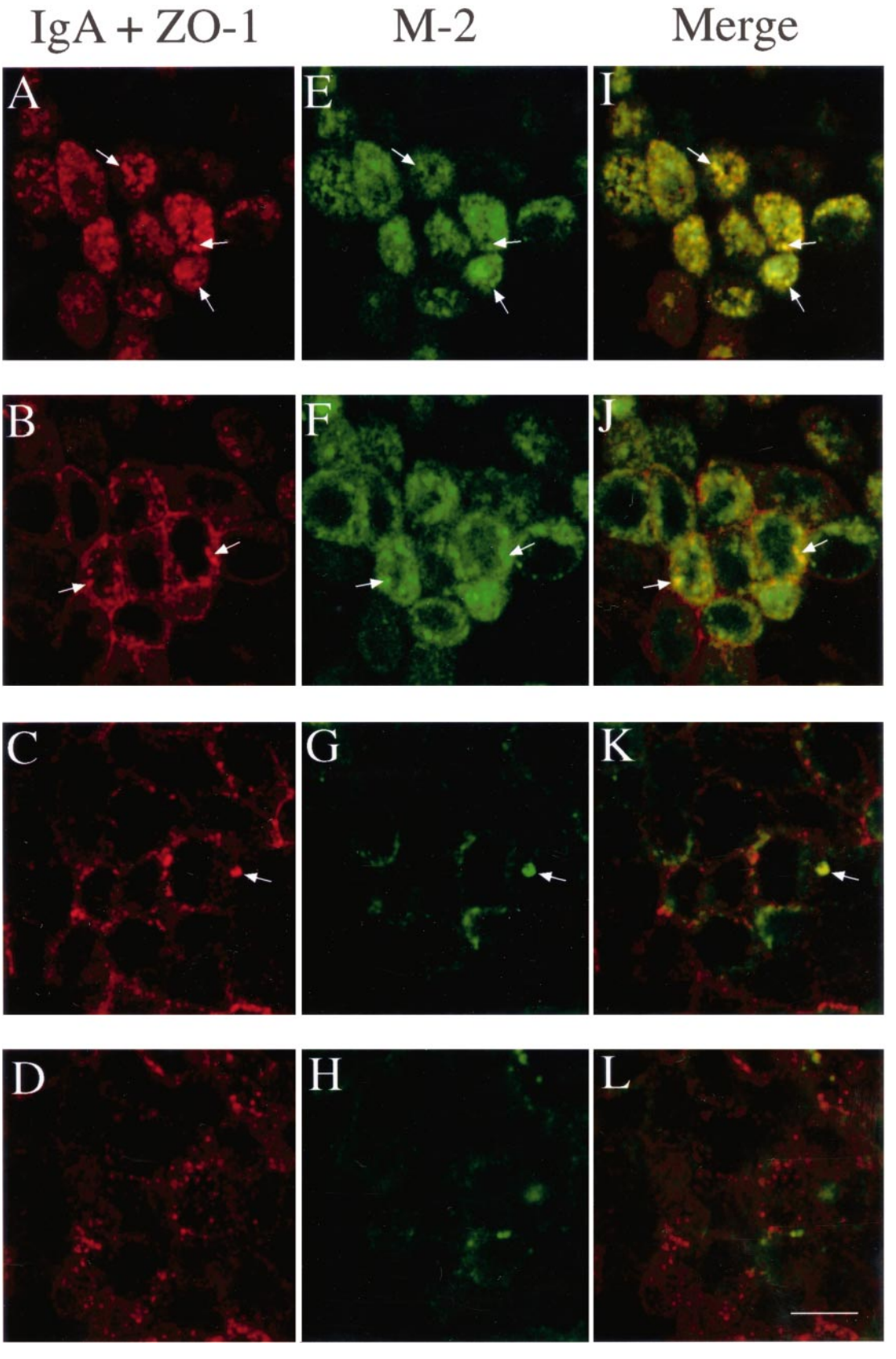

Figure 3.

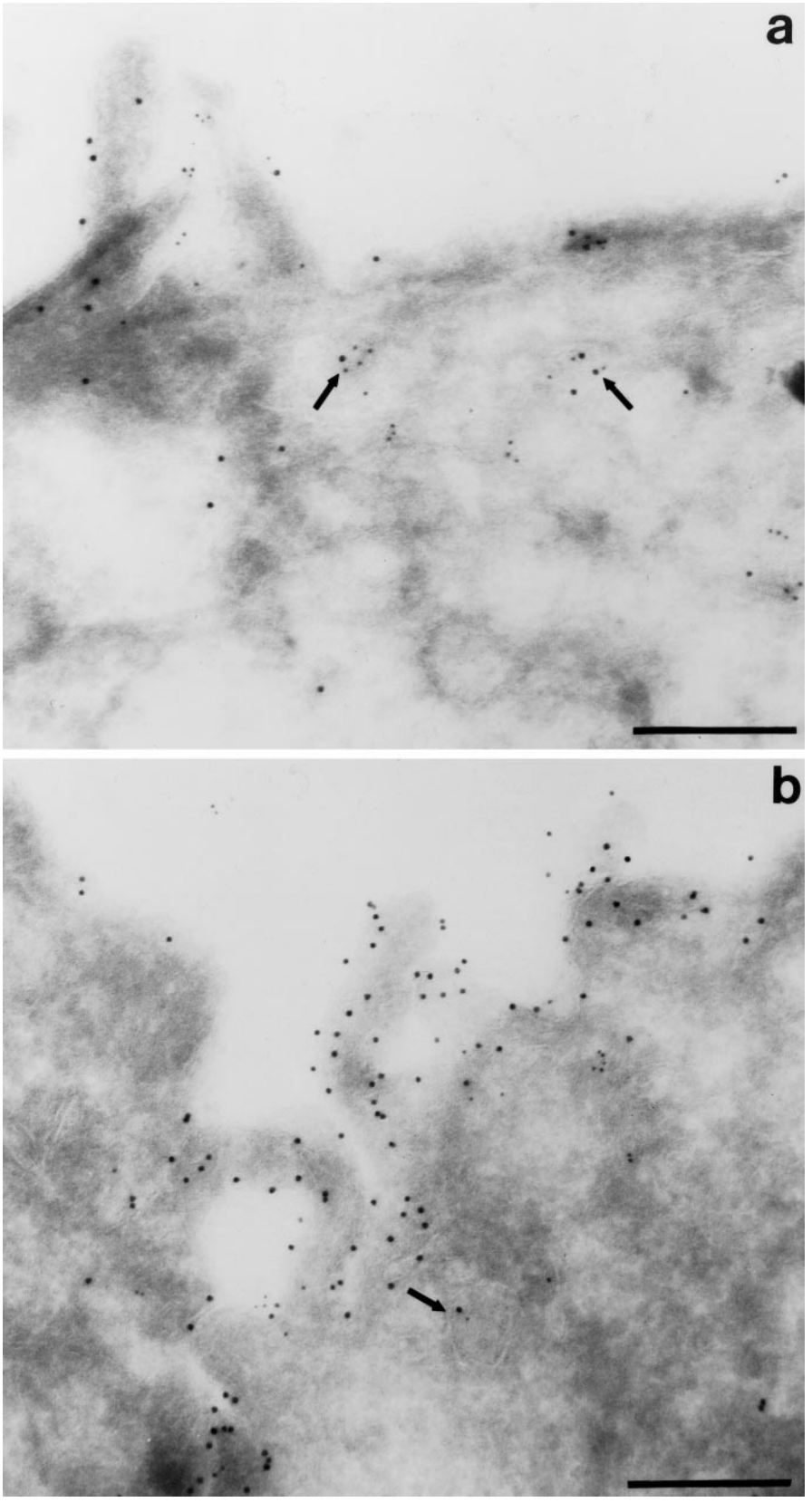

Figure 4. Colocalization of M2 and internalized IgA by indirect immunoelectron microscopy. Filter-grown T23 cells infected with AV-M2 were allowed to internalize IgA from the basolateral side for 10 min at 37°C and then washed extensively and chased for 3 min. Cells were then processed for double-label immunoelectron microscopy. M2 was detected using 10 nm gold, and IgA was localized using 5 nm gold. Subapical vesicles containing both M2 and IgA are marked with arrows. Bar, 0.25 μm.

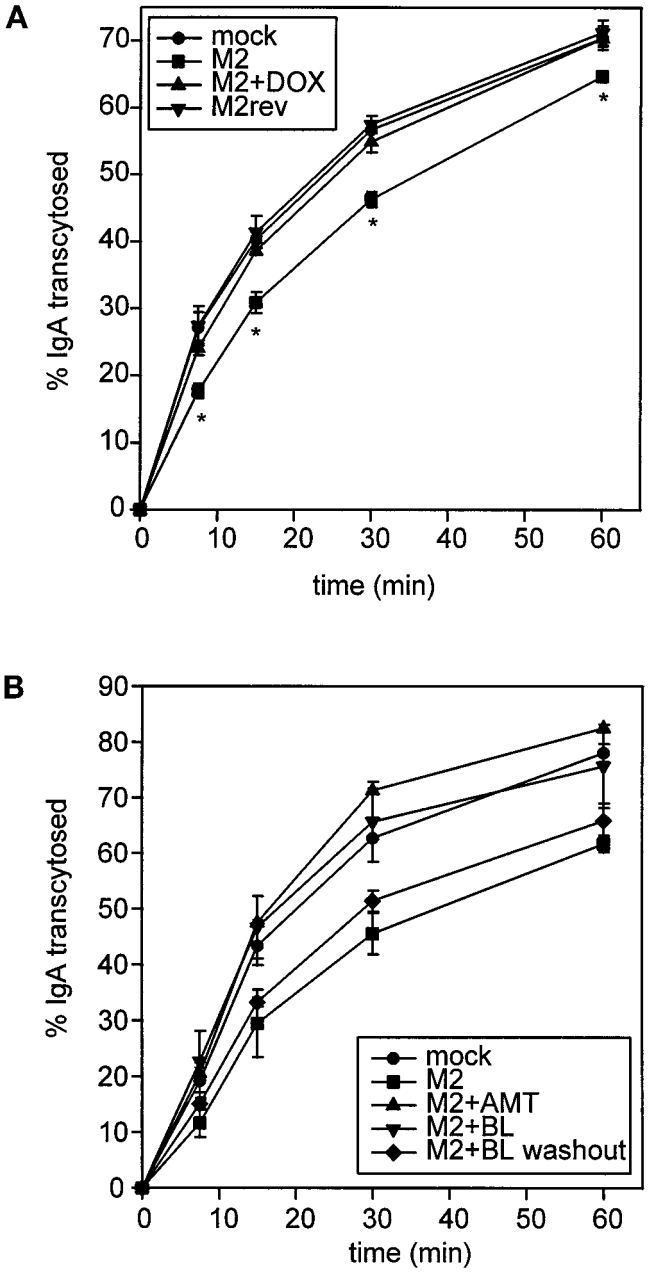

Figure 5. M2 slows the rate of basolateral-to-apical transcytosis of IgA. (A) Filter-grown MDCK T23 cells were mock infected or infected with AV-M2 or AV-M2rev and then treated with 2 mM butyrate (to induce pIgR synthesis) in the presence or absence of 20 ng/ml DOX. The next day, cells were incubated with basolaterally added [^{125}I]IgA at 37°C for 10 min and then washed extensively to remove free [^{125}I]IgA. After warming, the appearance of [^{125}I]IgA in the apical medium was monitored over a 1-h period. The mean ± SD from triplicate samples for each condition is shown. *, $p \leq 0.005$ compared with mock-infected controls. Similar results were observed in at least six experiments for each condition. (B) Filter-grown MDCK T23 cells were mock infected or infected with AV-M2, and the reversible M2 inhibitor BL-1743 (5 μM) was added to the indicated filters immediately after infection. The next day, filters were incubated for 30 min at 37°C in MEM/BSA before [^{125}I]IgA uptake. During this period, BL-1743 was washed out from some of the pretreated filters (M2+BL washout, diamonds), and AMT (5 μM) was added to some of the previously untreated filters (M2+AMT, triangles). The cells were then incubated with basolaterally added [^{125}I]IgA at 37°C for 10 min, and IgA transcytosis was monitored in the continued presence of BL-1743 (M2+BL, upside-down triangles) or AMT. The average ± range from duplicate samples is shown. Similar results were obtained in three experiments.

gether, these data support the idea that M2-mediated inhibition of IgA transcytosis is a rapid, direct, and reversible consequence of M2 ion channel activity in intracellular compartments.

Because transcytosis involves passage through both basolateral and apical endocytic compartments, we asked whether the effect of M2 was localized to a particular step in transport. Transcytosis from basolateral early endosomes to the ARE is microtubule dependent, and is inhibited by treatment with the microtubule-depolymerizing agent NOC. Thus by chasing IgA into the ARE and then blocking further transport into this compartment, we could determine whether M2 affected the transport of IgA from the ARE to the apical medium. Duplicate sets of filter-grown MDCK cells (mock infected or AV-M2 infected) were allowed to internalize [^{125}I]IgA for 10 min and then washed extensively at 0°C. The cells were then incubated at 37°C for 3 min to accumulate internalized IgA in the ARE. The filters were then rapidly chilled and treated with NOC for 60 min. After warming in the continued presence of NOC, release of IgA from the ARE into the apical medium was monitored. Under these conditions, the majority of microtubules in MDCK cells are depolymerized (Maples *et al.*, 1996). Expression of M2 decreased both the rate and extent of delivery of IgA from the ARE to the apical medium in the presence of NOC (Figure 6). The magnitude of the effect of M2 was similar to its effect on the rate of transcytosis in the presence of NOC (compare Figures 5A and 6). This suggests that transport from the ARE to the PM is the main step in transcytosis affected by active M2, consistent with our observation that intracellular M2 is concentrated at the apical pole of the cell. Furthermore, because the effect of M2 on transport occurs even when microtubules are depolymerized, this result demonstrates that the effect of M2 on transport is not due to altered interaction of vesicles with microtubules.

M2 Slows Apical but Not Basolateral Recycling

Because M2 slowed delivery of newly synthesized and transcytosing proteins to the apical surface, we asked whether M2 also affected apical recycling of preinternalized IgA (Figure 7A). This assay takes advantage of the small percentage of apically delivered pIgR that is

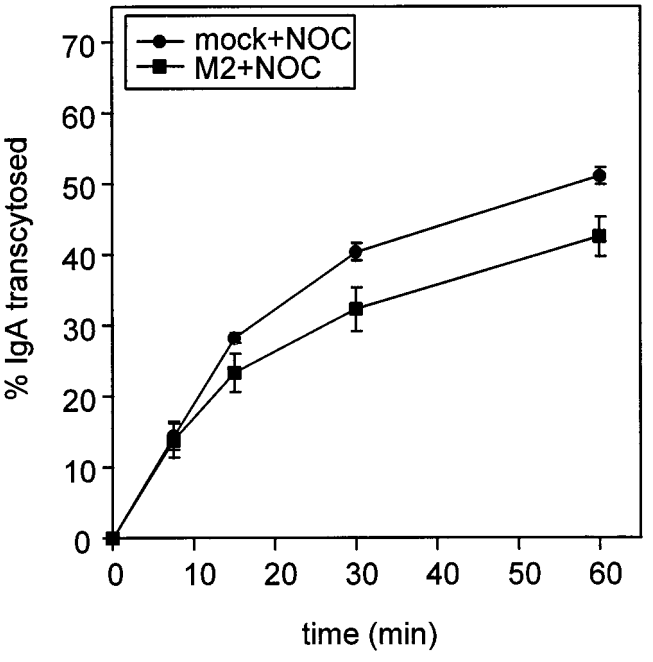

Figure 6. M2 blocks IgA transcytosis after the microtubule-dependent step. Filter-grown mock-infected or AV-M2-infected MDCK T23 cells were incubated with basolaterally added [^{125}I]IgA for 10 min and then rapidly chilled and washed extensively. The cells were then warmed to 37°C for 3 min to chase [^{125}I]IgA into the ARE, rapidly chilled, and incubated in NOC-containing medium on ice for 60 min. After warming in the continued presence of NOC, release of transcytosed [^{125}I]IgA into the apical medium was monitored as described above. The mean ± SD from triplicate samples is shown. Similar results were obtained in four experiments.

not proteolytically cleaved into the secretory component and is internalized and recycled at the apical domain. MDCK T23 cells infected with AV-M2 were incubated with apically added [^{125}I]IgA for 30 min and washed at 0°C, and reappearance of endocytosed IgA into the apical medium was monitored at 37°C. Expression of M2 caused a significant and reproducible lag in the initial rate of apical recycling of IgA compared with mock-infected cells, cells infected with AV-M2rev, or AV-M2-infected cells treated with DOX. The effect of M2 was not increased by infection with up to 10 times more AV-M2 and was completely reversed by inclusion of AMT or BL-1743 during the assay.

Although M2 had no effect on the amount of preinternalized IgA that recycles to the basolateral surface, we could not determine whether M2 altered the *rate* of recycling, because only a small fraction of preinternalized IgA returns to the basolateral surface. As such, we examined the effect of M2 on Tf, a marker of the basolateral recycling pathway (Figure 7B). Unlike IgA, internalized Tf is recycled to the basolateral surface with very high efficiency. Mock-infected or AV-M2-infected filter-grown MDCK cells were incubated with basolaterally added ^{125}I-labeled, iron-loaded Tf for 10 min and washed extensively, and basolateral recycling of the preendocytosed Tf was monitored. Recycling of this molecule to the basolateral surface was rapid and efficient (~90% of total) and was completely unaffected by M2 activity.

M2 Alters Protein Transport Selectively Compared with Global pH Perturbants

Because other perturbants of organelle pH have been demonstrated to alter protein trafficking in different systems, we compared the effects of M2 and the weak base ammonium chloride on postendocytic transport. Like M2 expression, treatment with 10 mM ammonium chloride inhibited ARE-to-PM transport of IgA (compare Figures 8A and 6). However, by contrast to M2, ammonium chloride treatment dramatically inhibited the release of basolaterally recycled Tf into the medium (Figure 8B). Similar results were obtained using Baf A_1 (0.5 μM). In addition, IgA degradation was typically inhibited by 50–70% in ammonium chloride–treated cells but not in M2-expressing cells. Together, these findings suggest that M2 selectively perturbs trafficking events at the apical surface.

DISCUSSION

We have expressed influenza M2 in polarized MDCK cells and examined its effect on apical and basolateral postendocytic transport. Unlike global pH perturbants, M2 expression selectively and reversibly perturbed protein transport through apical postendocytic compartments. Expression of active M2 altered the kinetics of IgA transcytosis and apical recycling but had no effect on protein degradation or on the rate of basolateral recycling of Tf. Our data provide the first demonstration that regulated acidification of the ARE is important for efficient delivery to the apical PM and provide a new method for studying the effect of acidification on individual transport steps.

Expression of M2 using a replication-defective recombinant adenovirus did not alter the morphology of polarized MDCK cells and did not affect the steady-state distribution of the apical marker influenza HA. In addition to its cell surface localization, M2 was found in subapical compartments. Intracellular M2 partly colocalized with transcytosing IgA in the ARE, and a small amount also colocalized with TGN-38. It is not clear whether M2 reaches the ARE via endocytosis from the PM or via another route. Some newly synthesized proteins have been shown to pass through endosomal compartments (including the ARE) en route to the PM (Futter *et al*., 1995; Aroeti and Apodaca, unpublished data). Although Rostock M2 contains the cytoplasmic sequence YRRL, which resembles adaptor-binding, tyrosine-based motifs involved

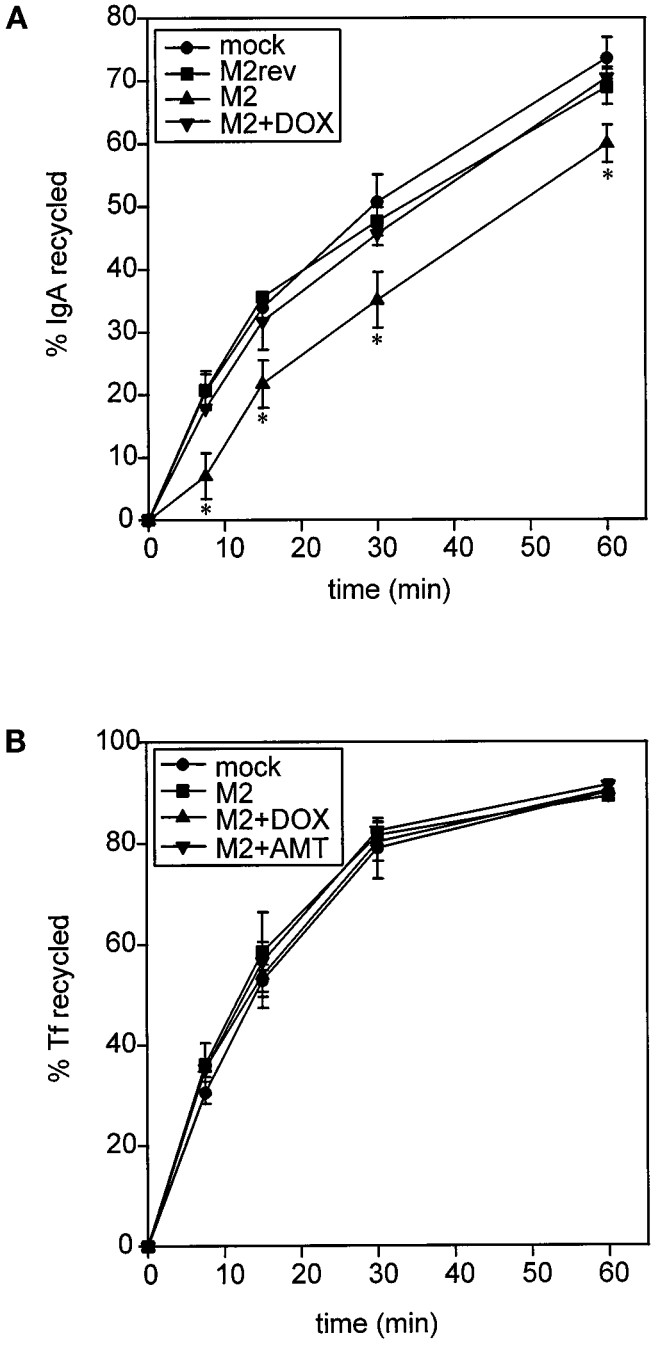

Figure 7. M2 expression affects apical but not basolateral recycling in polarized MDCK T23 cells. (A) MDCK T23 cells were mock infected or infected with AV-M2, and the indicated samples were treated with DOX overnight. Cells were incubated with apically added [^{125}I]IgA for 30 min and washed extensively at 0°C, and reappearance of endocytosed pIgA into the apical medium was monitored at 37°C. The average ± range from duplicate samples is plotted. *, $p < 0.05$ compared with mock-infected controls (data from 4 experiments compared using paired *t* test). (B) MDCK T23 cells infected as above were incubated with basolaterally added iron-loaded [^{125}I]Tf for 10 min and washed extensively, and basolateral recycling of the preendocytosed [^{125}I]Tf was monitored as described in MATERIALS AND METHODS. The mean ± SD from triplicate samples is shown. Similar results were obtained in four experiments.

in endocytosis, we found that M2 antibody bound to either PM domain was not rapidly internalized. In these experiments, a small amount of intracellular antibody could sometimes be detected, suggesting that M2 may be slowly internalized. We hypothesize that the tyrosine-containing motif in M2 is inaccessible to adaptor subunits, either because it is too close (eight amino acids) to the transmembrane domain to be efficiently recognized (Ohno *et al.*, 1996) or because M2 forms tetramers that could preclude binding of adaptor subunits.

Importantly, although the effects of M2 on apical delivery of preinternalized IgA were relatively modest (~35% reduction in initial rate), they are similar in magnitude to the effects of other pH perturbants on receptor trafficking through basolateral acidified compartments. Although many studies have examined the effects of pH perturbation on the recycling of iron-loaded Tf, the dramatic results observed using this assay reflect the pH dependence of iron dissociation from Tf rather than the pH dependence of the rate of Tf receptor trafficking. By contrast, we are most likely measuring the effects of M2 on pIgR trafficking. Recently, Presley *et al.* (1997) showed that Baf A_1 treatment causes a ~45% inhibition in the rate of Tf *receptor* recycling and a ~25% inhibition in the rate of bulk membrane return to the cell surface. Interestingly, the effects of pH perturbation on receptor recycling seem to be dependent on sorting signals in the protein cytoplasmic tails; the rate of recycling of a tailless mutant of the Tf receptor is unaffected by Baf A_1 (Johnson *et al.*, 1993; Presley *et al.*, 1997). Thus the modest effects of M2 on transcytosis and apical recycling we observed may suggest that efficient recognition of the sorting signals in the pIgR cytoplasmic tail is relatively insensitive to altered ARE pH.

Our data also suggest that M2 selectively perturbs the pH of only a subset of acidified compartments in the cell. In particular, M2 expression interfered with apical delivery of transcytosing and recycling molecules, consistent with the localization of intracellular M2 in subapical compartments. The effects of M2 on transcytosis were observed rapidly upon removal of the reversible M2 inhibitor BL-1743 and were blocked by addition of AMT shortly before IgA uptake, suggesting that M2-mediated changes in pH were directly responsible for the inhibition of IgA transport. Treatment with ammonium chloride and M2 had similar inhibitory effects on the rate of IgA release from the ARE to the apical PM in NOC-treated cells, suggesting that the effects of M2 on transport were due to altered endosomal pH. Together, our findings suggest that the

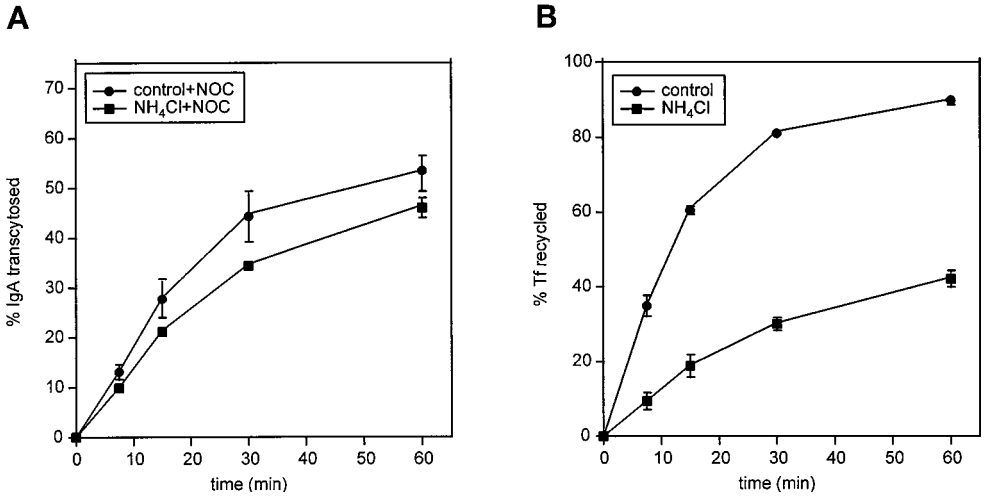

Figure 8. Ammonium chloride treatment affects multiple transport steps. Filter-grown T23 cells were incubated in MEM/BSA with or without 10 mM ammonium chloride for 30 min before [^{125}I]IgA or [^{125}I]Tf uptake. Assays were performed in the continued presence or absence of ammonium chloride as described in MATERIALS AND METHODS. (A) ARE-to-PM release of IgA from NOC-treated cells treated with or without ammonium chloride. (B) Tf recycling in control versus ammonium chloride-treated cells.

ARE is normally acidified, and that acidification is important for efficient sorting of itinerant molecules in this compartment. Further work to quantitate the effect of M2 on the pH of the ARE is currently under way.

The effects of M2 on some steps in postendocytic transport were different from those observed by us and others using global perturbants, which alter the pH of all acidified compartments. For example, M2 expression did not affect the degradation of preinternalized IgA, suggesting that M2 is not present in lysosomal compartments. By contrast, IgA degradation was dramatically inhibited in ammonium chloride–treated cells. In addition, treatment with ammonium chloride or Baf A_1 significantly affected the rate of basolateral release of preinternalized Tf, whereas M2 expression had no effect on basolateral recycling of either IgA or Tf. This finding clearly demonstrates that M2 expression does not significantly alter the pH of basolateral sorting endosomes, where dissociation of iron from Tf is thought to occur. It is also consistent with our observation that very little M2 was found in basolateral early endosomes.

We can envision several ways in which M2-mediated perturbation of organelle pH could alter protein traffic through a compartment. One idea is that blocking acidification may interfere with coat protein binding at the cytoplasmic face of compartment. In support of this hypothesis, Aniento *et al.* (1996) have obtained evidence that β and ϵ COP binding to endosomal membranes is abolished in the presence of Baf A_1. This finding suggests that acidified compartments contain a transmembrane pH sensor that regulates cytosolic coat formation. However, the dramatic results they obtained in their in vitro system are difficult to reconcile with the more modest effects of Baf A_1 and other drugs on transport in intact cells (Johnson *et al.*, 1993; van Weert *et al.*, 1995; Presley *et al.*, 1997). A related hypothesis is that acidification may be required for the proper association of sorting organelles with the cytoskeleton. In separate studies, disruption of either cytoplasmic or vesicular pH altered endosomal morphology and interaction with microtubules (Parton *et al.*, 1991; D'Arrigo *et al.*, 1997). Microtubule-induced changes in endosome shape could play an important role in their ability to segregate components efficiently. However, M2 activity slowed IgA delivery to the apical surface even in the presence of NOC, suggesting that the effects of M2 on transport are microtubule independent. Another possibility is that acidification is important for an enzymatic activity (e.g., lipid synthesis) required for efficient vesicle formation in acidified compartments or for cargo clustering into forming vesicles. Recent studies demonstrating that Baf A_1 slows recycling of the Tf receptor via a mechanism involving the tyrosine-based internalization motif on the receptor's cytoplasmic tail (Johnson *et al.*, 1993; Presley *et al.*, 1997) support the idea that loading of cargo into vesicles is pH dependent. Finally, acidification could play different roles in distinct compartments; for example, the function of acidification in TGN sorting could be different than in endosomal sorting.

Together, our data suggest that M2 expression disrupts the acidification of apical but not basolateral postendocytic compartments. The kinetics of transcytosis and apical recycling are selectively slowed by expression of the influenza ion channel M2, whereas basolateral recycling is unaffected by M2 activity. Use of global perturbants to alter the pH of all acidified compartments has yielded inconclusive and conflicting data about the role of acidification in biosynthetic and endocytic traffic, probably because multiple transport pathways and metabolic processes are altered. By contrast, M2 expression and activity can be manipulated to reversibly affect pH in only a subset of acidi-

fied compartments and may thus allow dissection of the role of acidification in individual transport steps without these complications. We anticipate that site-directed mutagenesis could be used to relocate M2 within polarized cells, allowing us to examine the effect of M2 expression on transport through other acidified compartments.

ACKNOWLEDGMENTS

We thank Wily Geovany Ruiz for expert assistance with the immunoelectron microscopy, Robert Lamb for his generous gifts of cDNA encoding Rostock M2 and anti-M2 antibodies, Michael Roth for cDNA encoding HA_{Japan}, Thomas Braciale for the Fc125 hybridoma cell line, Mark Krystal for supplying BL-1743, and Kenneth Dunn and Rebecca Hughey for helpful discussions and critical review of the manuscript. This work was supported in part by Dialysis Clinic Inc. and by grants from the Cystic Fibrosis Foundation and the Competitive Medical Research Fund of the University of Pittsburgh Medical Center (to O.A.W.). These experiments were performed during the tenure of an American Heart Association Minority Development Award and a grant from National Institutes of Health (R01DK51970-01) to G.A.

REFERENCES

Aniento, F., Gu, F., Parton, R.G., and Gruenberg, J. (1996). An endosomal βCOP is involved in the pH-dependent formation of transport vesicles destined for late endosomes. J. Cell Biol. *133*, 29–41.

Apodaca, G., Cardone, M.H., Whiteheart, S.W., DasGupta, B.R., and Mostov, K.E. (1996). Reconstitution of transcytosis in SLO-permeabilized MDCK cells: existence of an NSF-dependent fusion mechanism with the apical surface of MDCK cells. EMBO J. *15*, 1471–1481.

Apodaca, G., Katz, L.A., and Mostov, K.E. (1994). Receptor-mediated transcytosis of IgA in MDCK cells is via apical recycling endosomes. J. Cell Biol. *125*, 67–86.

Barth, A.I.M., Pollack, A.L., Altschuler, Y., Mostov, K.E., and Nelson, W.J. (1997). NH_2-terminal deletion of β-catenin results in stable colocalization of mutant β-catenin with adenomatous polyposis coli protein and altered MDCK cell adhesion. J. Cell Biol. *136*, 693–706.

Bomsel, M., Prydz, K., Parton, R.G., Gruenberg, J., and Simons, K. (1989). Endocytosis in filter-grown Madin-Darby canine kidney cells. J. Cell Biol. *109*, 3243–3258.

Breitfeld, P.P., Casanova, J.E., Harris, J.M., Simister, N.E., and Mostov, K.E. (1989a). Expression and analysis of the polymeric immunoglobulin receptor in Madin-Darby canine kidney cells using retroviral vectors. Methods Cell Biol. *32*, 329–337.

Breitfeld, P.P., Casanova, J.E., McKinnon, W.C., and Mostov, K.E. (1990). Deletions in the cytoplasmic domain of the polymeric immunoglobulin receptor differentially affect endocytotic rate and postendocytotic traffic. J. Biol. Chem. *265*, 13750–13757.

Breitfeld, P.P., Harris, J.M., and Mostov, K.E. (1989b). Postendocytic sorting of the ligand for the polymeric immunoglobulin receptor in Madin-Darby canine kidney cells. J. Cell Biol. *109*, 475–486.

Clague, M.J., Urbe, S., Aniento, F., and Gruenberg, J. (1994). Vacuolar ATPase activity is required for endosomal carrier vesicle formation. J. Biol. Chem. *269*, 21–24.

D'Arrigo, A., Bucci, C., Toh, B.-H., and Stenmark, H. (1997). Microtubules are involved in bafilomycin A1-induced tubulation and Rab5-dependent vacuolation of early endosomes. Eur. J. Cell Biol. *72*, 95–103.

Duff, K.C., and Ashley, R.H. (1992). The transmembrane domain of influenza A M2 protein forms amantadine-sensitive proton channels in planar lipid bilayers. Virology. *190*, 485–489.

Futter, C.E., Connolly, C.N., Cutler, D.F., and Hopkins, C.R. (1995). Newly synthesized transferrin receptors can be detected in the endosome before they appear on the cell surface. J. Biol. Chem. *270*, 10999–11003.

Gossen, M., and Bujard, H. (1992). Tight control of gene expression in mammalian cells by tetracycline-responsive promoters. Proc. Natl. Acad. Sci. USA *89*, 5547–5551.

Grambas, S., and Hay, A.J. (1992). Maturation of influenza A virus hemagglutinin- estimates of the pH encountered during transport and its regulation by the M2 protein. Virology *190*, 11–18.

Green, M., and Pina, M. (1963). Biochemical studies on adenovirus multiplication. Virology *20*, 199–207.

Hardy, S., Kitamura, M., Harris-Stansil, T., Dai, Y., and Phipps, M.L. (1997). Construction of adenovirus vectors through Cre-*lox* recombination. J. Virol. *71*, 1842–1849.

Henkel, J.R., and Weisz, O.A. (1998). Influenza virus M2 protein slows traffic along the secretory pathway: pH perturbation of acidified compartments affects early Golgi transport steps. J. Biol. Chem. *273*, 6518–6524.

Johnson, L.S., Dunn, K.W., Pytowski, B., and McGraw, T.E. (1993). Endosome acidification and receptor trafficking: Bafilomycin A_1 slows receptor externalization by a mechanism involving the receptor's internalization motif. Mol. Biol. Cell *4*, 1251–1266.

Lamb, R.A., and Choppin, P.W. (1981). Identification of a second protein (M_2) encoded by RNA segment of influenza virus. Virology *112*, 729–737.

Maples, C.J., Ruiz, W.G., and Apodaca, G. (1996). Both microtubules and actin filaments are required for efficient postendocytic traffic of the polymeric immunoglobulin receptor in polarized Madin-Darby canine kidney cells. J. Biol. Chem. *272*, 6741–6751.

Muroi, M., Shiragami, N., Nagao, K., Yamasaki, M., and Takatsuki, A. (1993). Folimycin (concanamycin A), a specific inhibitor of V-ATPase, blocks intracellular translocation of the glycoprotein of vesicular stomatitis virus before arrival to the Golgi apparatus. Cell Struct. Funct. *18*. 139–149.

Ohno, H., Fournier, M.-C., Poy, G., and Bonifacino, J.S. (1996). Structural determinants of interaction of tyrosine-based sorting signals with the adaptor medium chains. J. Biol. Chem. *271*, 29009–29015.

Palokangas, H., Metsikko, K., and Vaananen, K. (1994). Active vacuolar H^+ATPase is required for both endocytic and exocytic processes during viral infection of BHK-21 cells. J. Biol. Chem. *269*, 17577–17585.

Parton, R.G., Dotti, C.G., Bacallao, R., Kurtz, I., Simons, K., and Prydz, K. (1991). pH-induced microtubule-dependent redistribution of late endosomes in neuronal and epithelial cells. J. Cell Biol. *113*, 261–274.

Pinto, L.H., Holsinger, L.J., and Lamb, R.A. (1992). Influenza virus M_2 protein has ion channel activity. Cell *69*, 517–528.

Presley, J.F., Mayor, S., McGraw, T.E., Dunn, K.W., and Maxfield, F.R. (1997). Bafilomycin A_1 treatment retards transferrin receptor recycling more than bulk membrane recycling. J. Biol. Chem. *272*, 13929–13936.

Sakaguchi, T., Leser, G.P., and Lamb, R.A. (1996). The ion channel activity of the influenza virus M_2 protein affects transport through the Golgi apparatus. J. Cell Biol. *133*, 733–747.

Sugrue, R.J., and Hay, A.J. (1991). Structural characteristics of the

M2 protein of influenza A viruses: evidence that it forms a tetrameric channel. Virology *180*, 617–624.

Tu, Q., Pinto, L.H., Luo, G., Shaughnessy, M.A., Mullaney, D., Kurtz, S., Krystal, M., and Lamb, R.A. (1996). Characterization of inhibition of M_2 ion channel activity by BL-1743, an inhibitor of influenza A virus. J. Virol. *70*, 4246–4252.

van Weert, A.W.M., Dunn, K.W., Geuze, H.J., Maxfield, F.R., and Stoorvogel, W. (1995) Transport from late endosomes to lysosomes, but not sorting of integral membrane proteins in endosomes, depends on the vacuolar proton pump. J. Cell Biol. *130*, 821–834.

Yilla, M., Tan, A., Ito, K., Miwa, K., and Ploegh, H.L. (1993). Involvement of the vacuolar H^+-ATPases in the secretory pathway of HepG2 cells. J. Biol. Chem. *268*, 19092–19100.

Yoshimori, T., Yamamoto, A., Moriyama, Y., Futai, M., and Tashiro, Y. (1991). Bafilomycin A_1, a specific inhibitor of vacuolar-type H^+ATPase, inhibits acidification and protein degradation in lysosomes of cultured cells. J. Biol. Chem. *266*, 17707–17712.

Zebedee, S.L., Richardson, C.D., and Lamb, R.A. (1985). Characterization of the influenza virus M_2 integral membrane protein and expression at the infected-cell surface from cloned cDNA. J. Virol. *56*, 502–511.